Supplementary Information

Table of contents: **Pages:**

Supplementary Table 1-3 in separate files

Supplementary Methods

RNAPII ChIP (detailed methods):

Cells were crosslinked with 1% formaldehyde for 20 min at room temperature. The reaction was quenched with glycine and the cells were successively washed with phosphate-buffered saline, buffer B [0.25% Triton-X 100, 10mM ethylenediaminetetraacetic acid (EDTA), 0.5 mM ethylene glycol tetraacetic acid (EGTA), 20mM HEPES (pH 7.6)] and buffer C [0.15M NaCl, 1mM EDTA, 0.5mM EGTA, 20mM HEPES (pH 7.6)]. The cells were then resuspended in ChIP incubation buffer [0.3% sodium dodecyl sulfate (SDS), 1% Triton-X 100, 0.15 M NaCl, 1mM EDTA, 0.5mM EGTA, 20mM HEPES (pH 7.6)] and sheared using Biorupter Sonicator. The sonicated chromatin was diluted to 0.15% SDS, incubated for 16h at 4°C with 10µl of the anti RBP1 per IP with 100µl of protein A/G beads. All buffers contained Roche protease inhibitor cocktail. The beads were successively washed two times with buffer 1 [0.1% SDS, 0.1% deoxycholate, 1% Triton-X 100, 0.15M NaCl, 1mM EDTA, 0.5mM EGTA, 20mM HEPES (pH 7.6)], one time with buffer 2 [0.1% SDS, 0.1% sodium deoxycholate, 1% Triton-X 100, 0.5M NaCl, 1mM EDTA, 0.5mM EGTA, 20mMHEPES (pH 7.6)], one time with buffer 3 (0.25M LiCl, 0.5% sodium deoxycholate, 0.5% NP-40, 1mM EDTA, 0.5mM EGTA, 20mM HEPES (pH 7.6)], and two times with buffer 4 (1mM EDTA, 0.5mM EGTA, 20mM HEPES (pH 7.6)] for 5 min each at 4°C. Chromatin was eluted by incubation of the beads with elution buffer (1% SDS, 0.1M NaHCO3) at room temperature, the eluted fraction was de-cross-linked by incubation at 65°C for 16h in the presence of 200mM NaCl, extracted with phenol–chloroform-isoamyl, and ethanol precipitated.

FOXO3 and histone ChIPs (detailed methods):

Cells were cross-linked with formaldehyde (1%) for 10 min at room temperature and incubated with glycine (0.125M) for 5 min. Cells were washed with PBS and lysed in Farnham lysis buffer (5mM PIPES, 85mM KCl, 0.5%NP-40, protease inhibitor cocktail Roche). Nuclear extracts were collected by centrifuging at 2000 rpm. for 5 min. The cell nuclei were re-suspended in RIPA buffer (1xPBS, 1% NP-40, 0.5% Na-deoxycholate, 0.1% SDS, supplemented with Roche protease inhibitor cocktail). Chromatin was sonicated with a Bioruptor sonicator. Chromatin extracts were pre-cleared for 1 hour and subsequently incubated for 16h with beads and antibody. For FOXO3 ChIPs, beads were washed five times with RIPA buffer. For histone modifications, beads were washed twice in 1ml low-salt ChIP buffer (0.1% SDS, 1% Triton X-100,2mM EDTA, 20mM Tris–HCl, pH 8.1, 150mM NaCl), two times in 1ml high-salt ChIP buffer (0.1% SDS, 1% TritonX-100, 2mM EDTA, 20mM Tris–HCl, pH 8.1, 500mMNaCl), two times with 1ml LiCl ChIP buffer (0.25M LiCl,1% IGEPAL CA630, 1% deoxycholic acid (sodium salt), 1mMEDTA, 10mM Tris, pH 8.1), and once in TE buffer. Chromatin was eluted by incubation of the beads with elution buffer (1% SDS, 0.1M NaHCO3). The eluted fraction was de-cross-linked by incubation at 65°C for 5 to 16h in the presence of 200mM NaCl, extracted with phenol–chloroform-isoamyl, and ethanol precipitated.

RNA purification and cDNA synthesis:

DLD1-F3, DLD1-DBD and DLD1 cells were treated for 8 hours and RNA was purified with RNeasy kit (Qiagen). cDNA was synthesized using iScript cDNA synthesis kit (Biorad). qPCR analysis was performed with IQ SYBR-Green mix (Biorad), primer sequences in Table S3.

Supplementary Figure 1:

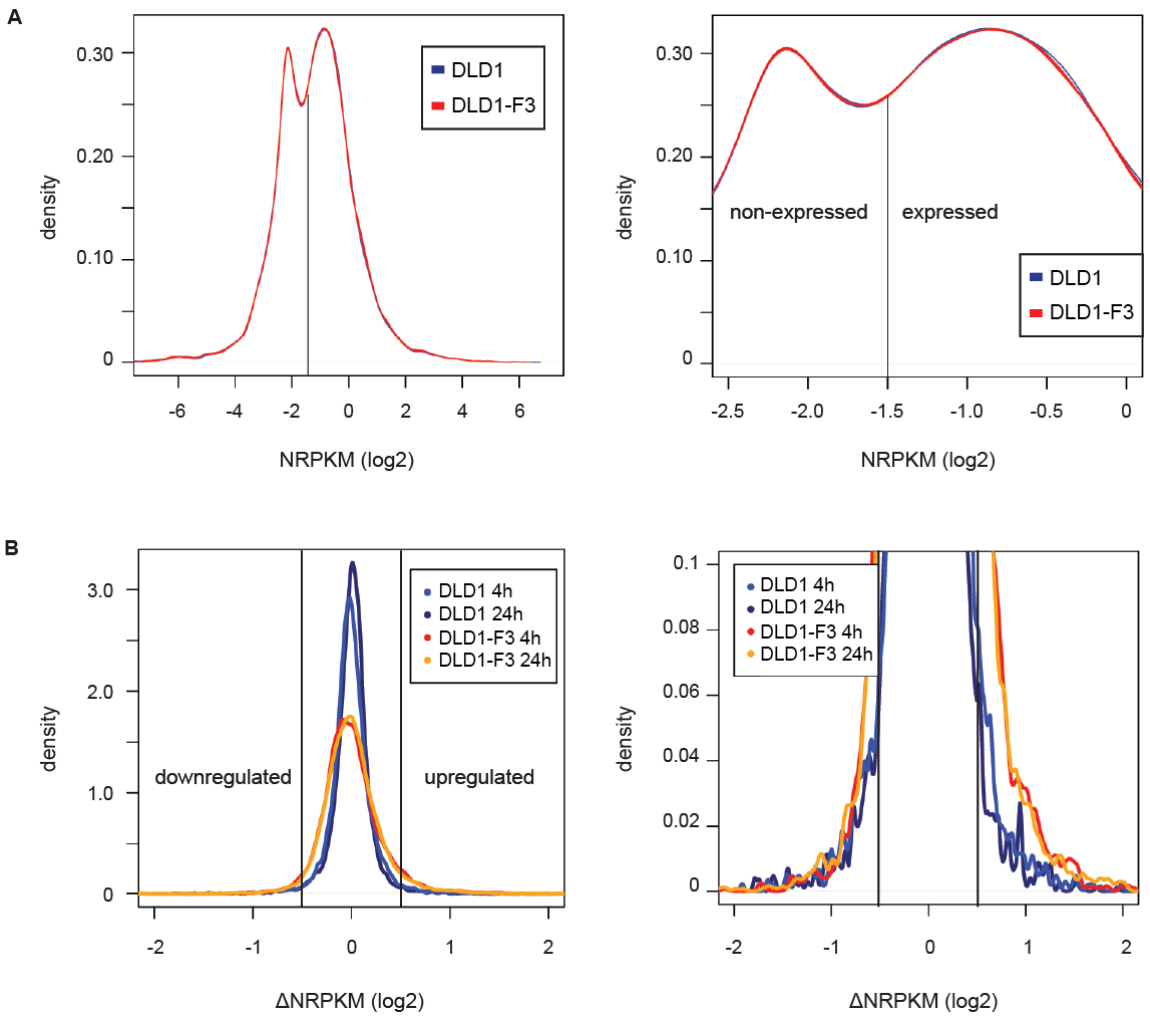

Determination of cut-off values for RNAPII quantification. (**A**) The overall distribution of RNAPII occupancy in normalized number of reads per kb per million of reads (NRPKM). Distribution is bimodal (suggests on and off pool of genes) and nearly identical in DLD1 and DLD1-F3. -1.5 RPKM (log2) is the cut-off used for expression. (**B**) The overall distribution of the change in RNAPII occupancy upon addition of 4OHT in DLD1-F3 and DLD1 cells. More changes are occurring in DLD1-F3 compared with DLD1. Changes in DLD1 were used to estimate the background in DLD1-F3 samples, which resulted in a cut-off of 0.5 (log2). Genes with over 0.2 fold changes in DLD1 cells were excluded from further analysis.

Supplementary Figure 2:

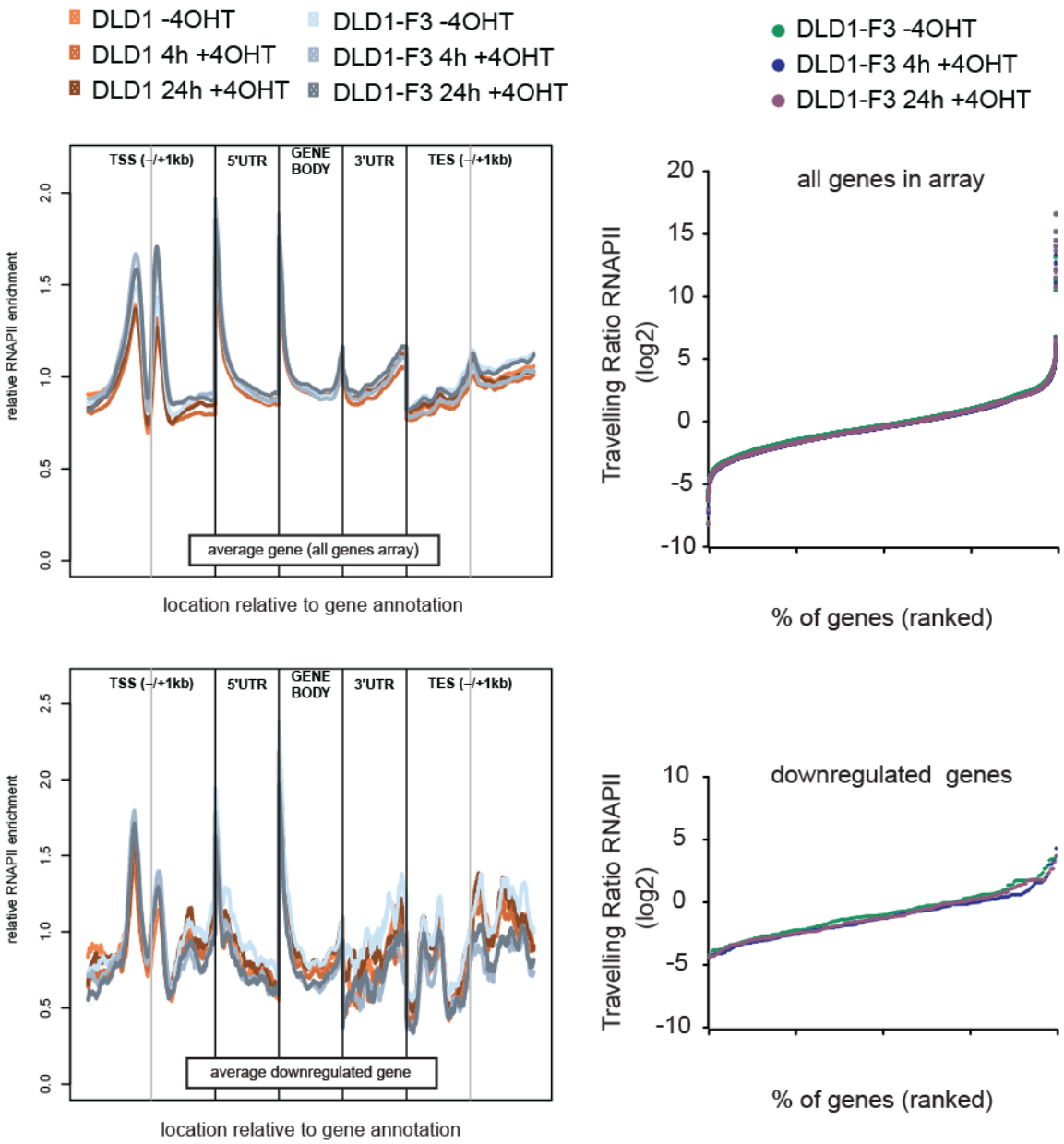

Meta-gene analysis of RNAPII occupancy in all genes and downregulated genes only, which were specified by changes in micro-array analysis. Genes were divided into 1kb regions surrounding TSS and TES, and gene-size adjusted 5`UTR, 3`UTR and gene body, with separate normalization. The profile (left) is shown for DLD1 and DLD1-F3, untreated, 4h and 24h upon addition of 4OHT. Travelling ratio was determined for the same gene sets (right), ranked by increasing ratio for DLD1-F3 untreated, 4h and 24h treated separately.

Supplementary Figure 3:

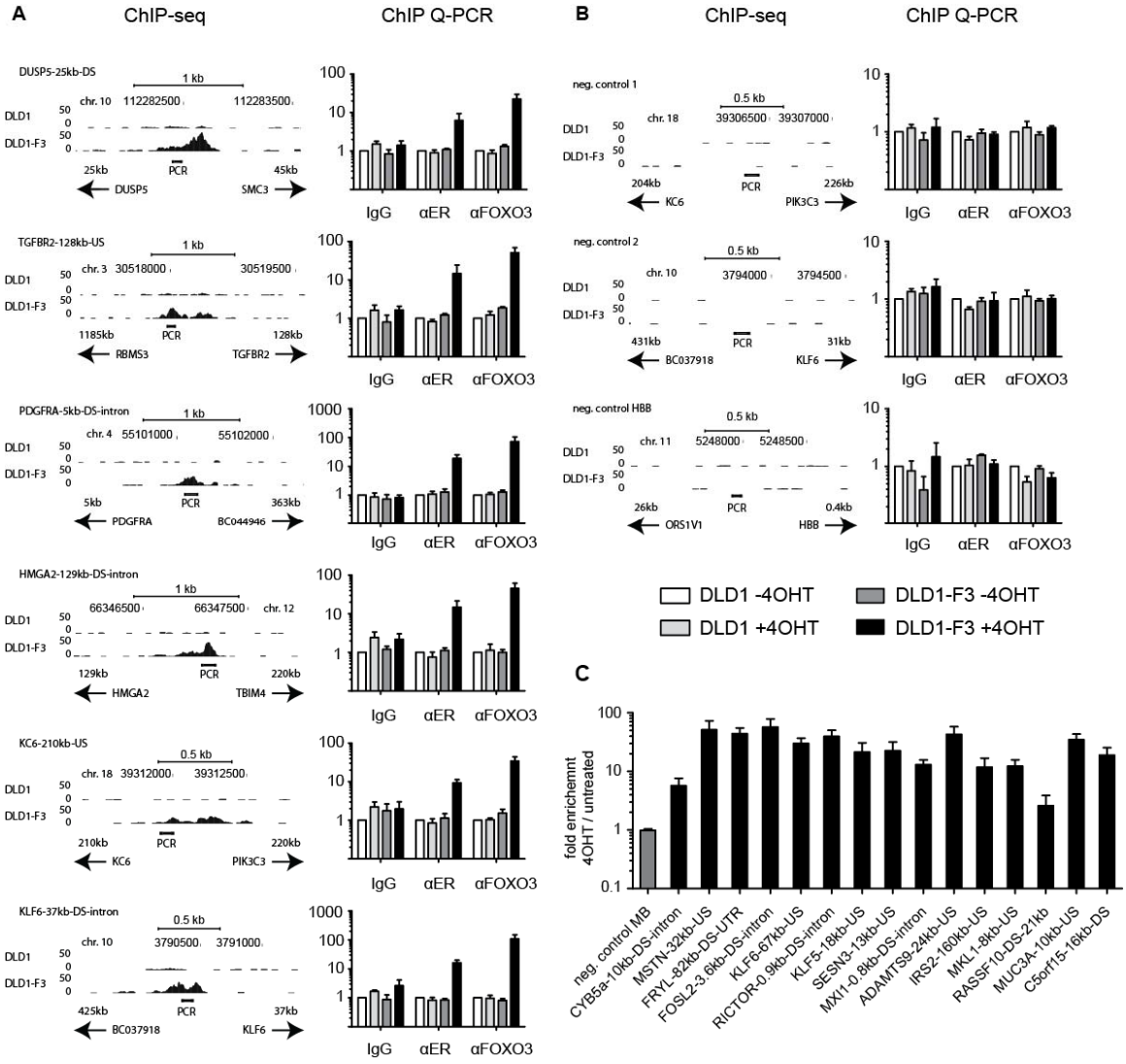

Confirmation of FOXO3 ChIP-seq binding profile. (**A**) Six peaks and surrounding genomic regions in DLD1 and DLD1-F3, including location, scale, distance to nearest upstream and downstream gene TSS, and PCR amplicon. ChIP-qPCR performed with αFOXO3, αER and IgG, fold change relative to DLD1 untreated signal is shown (three biological replicates, mean and SEM). Peaks are named according to closest TSS, with distance and location relative to TSS (US upstream, DS downstream) and if located within intron. (**B**) Three control regions without FOXO3 binding, of which neg. control 1 and neg. control 2 are 5 kb upstream from peak KC6-210kb-US and KLF6-37kb-DS-intron and HBB is within *HBB*. (**C**) Fifteen additional peaks were tested for induction by 4OHT in DLD1-F3 cells (two biological replicates, mean and SEM).

Supplementary Figure 4:

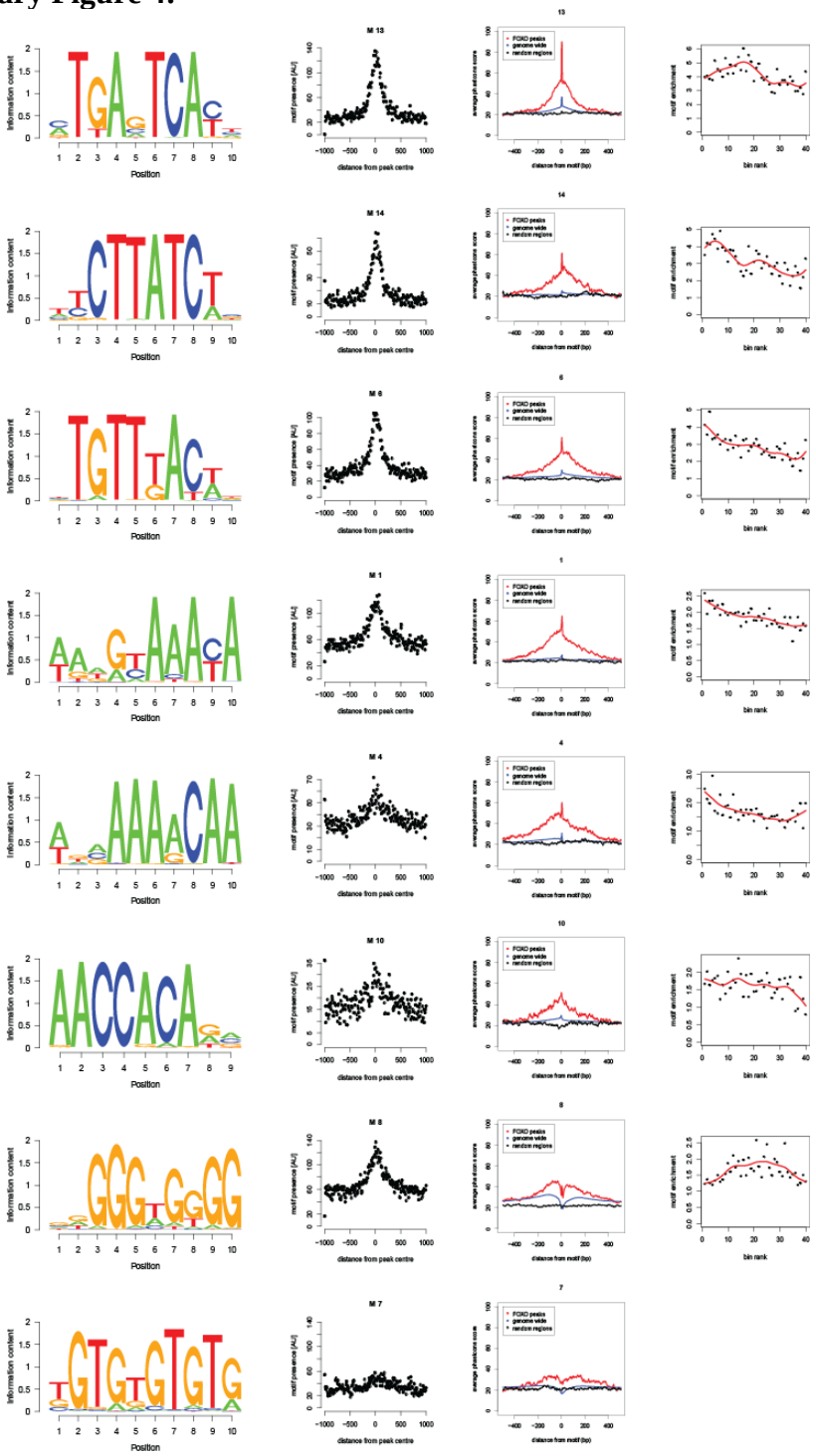

Analysis of candidate binding motifs in FOXO3 peaks. De novo motif search resulted in eight motifs, of which seven found with increased presence around the peak centre. From left to right: motif, presence relative to peak centre (region with highest number of reads), conservation of the motif and surrounding regions in FOXO3 bound regions compared with genome-wide motif conservation and random regions, presence in peaks ranked from high to low. The last motif was excluded because of random distribution relative to peak centre and simple repeat resemblance.

Supplementary Figure 5:

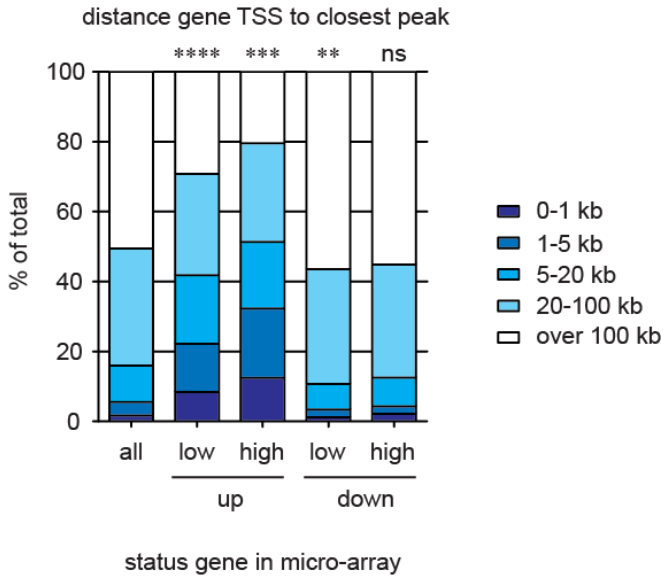

Positive correlation between FOXO3 binding and upregulation of mRNA levels. Comparison of the gene status in micro-array expression analysis and the distance between the gene TSS and closest FOXO3 peak. The distribution of all genes present in array is shown, as well as significantly up- and downregulated genes divided in low (1.3 fold) and high (2.0 fold). Hypergeometric test for number of genes with peak within 20kb of subsets versus all (ns = $p>0.05$, * = $p<0.05$, ** = $p<5•10\text{-}5$, *** = $p<5•10\text{-}15$, **** = $p<5•10\text{-}30$).

Supplementary Figure 6:

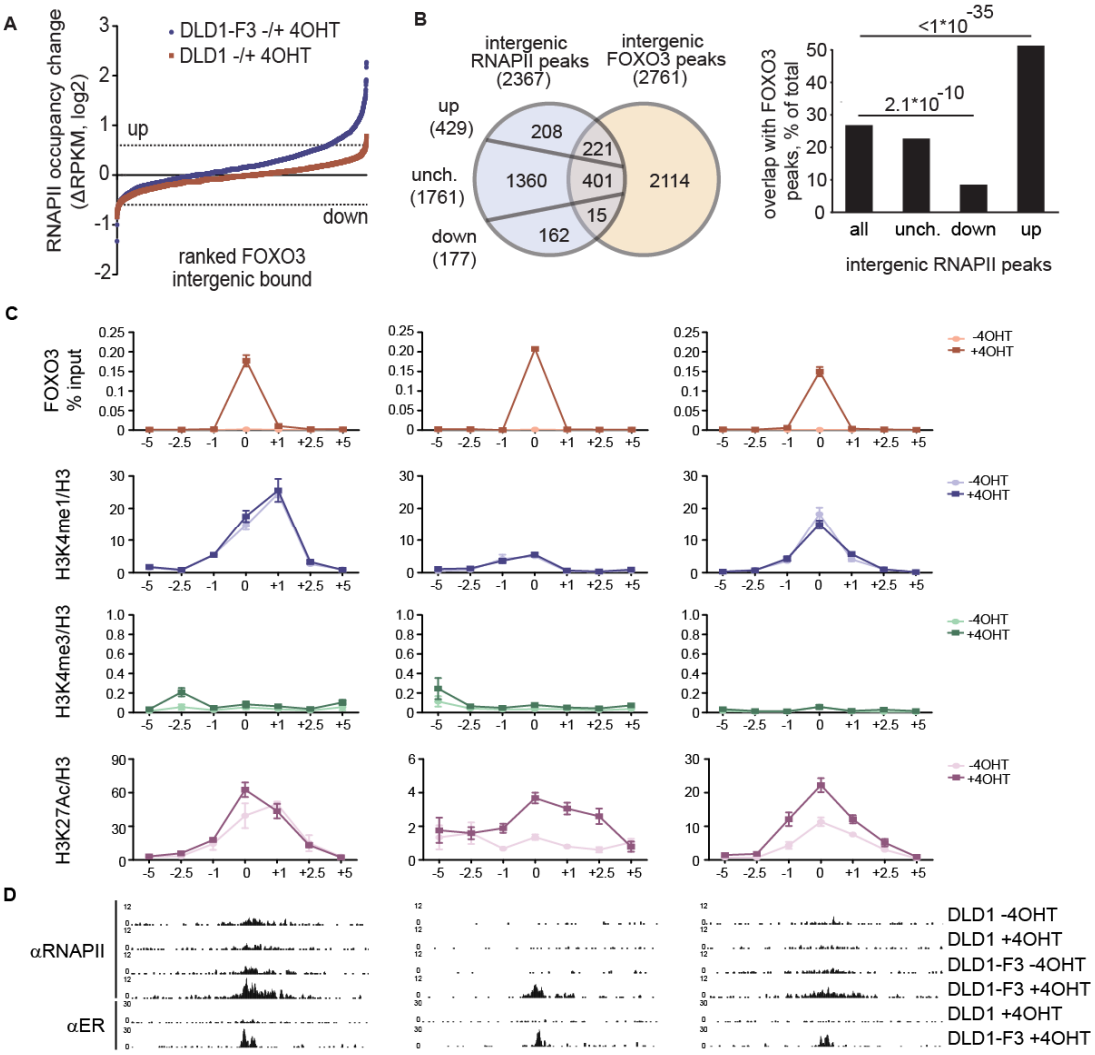

FOXO3 binds to and activates enhancers. (**A**) Changes in RNAPII occupancy (ΔRPKM) for all intergenic FOXO3 regions in DLD1 and DLD1-F3 cells (4h versus untreated), sorted for increasing value. Changes at FOXO3 bound regions in DLD1 cells are used to estimate noise and determine cut-off (0.6 fold). (**B**) Overlap between up, unchanged (unch.) or downregulated intergenic RNAPII peaks (4h versus untreated) and FOXO3 intergenic peaks. Overlap is shown in Venn diagram and percentage of total RNAP II peaks (p-value from hypergeometric test). (**C**) ChIPs on DLD1-F3 cells (not treated and treated with 4OHT for 2 hours) with antibodies recognizing FOXO3, H3K4me1, H3K4me3, H3K27Ac and H3. Immunoprecipitated DNA was analyzed by qPCR for three FOXO3 bound regions (TGFBR2-128kb-upstream, PDGFRA-5kb-downstream- intron, KC6-210kb-upstream), with 0 denoting the peak centre and surrounding regions located 1, 2.5 and 5kb up- and downstream from peak centre. The enrichment for modifications over total H3 is calculated (three technical replicates, average with SD). For comparison, enrichment for H3K4me1, H3K4me3 and H3K27Ac over H3 was 12, 8.9 and 74 fold respectively at GAPDH control region. (**D**) RNAPII and FOXO3 browser views for 10kb regions surrounding the same FOXO3 bound regions. A local increase in RNAPII around the FOXO3 bound region can be observed upon FOXO3 activation (only 4h treatment is shown, 24h profiles resemble 4h profiles).

Supplementary Figure 7:

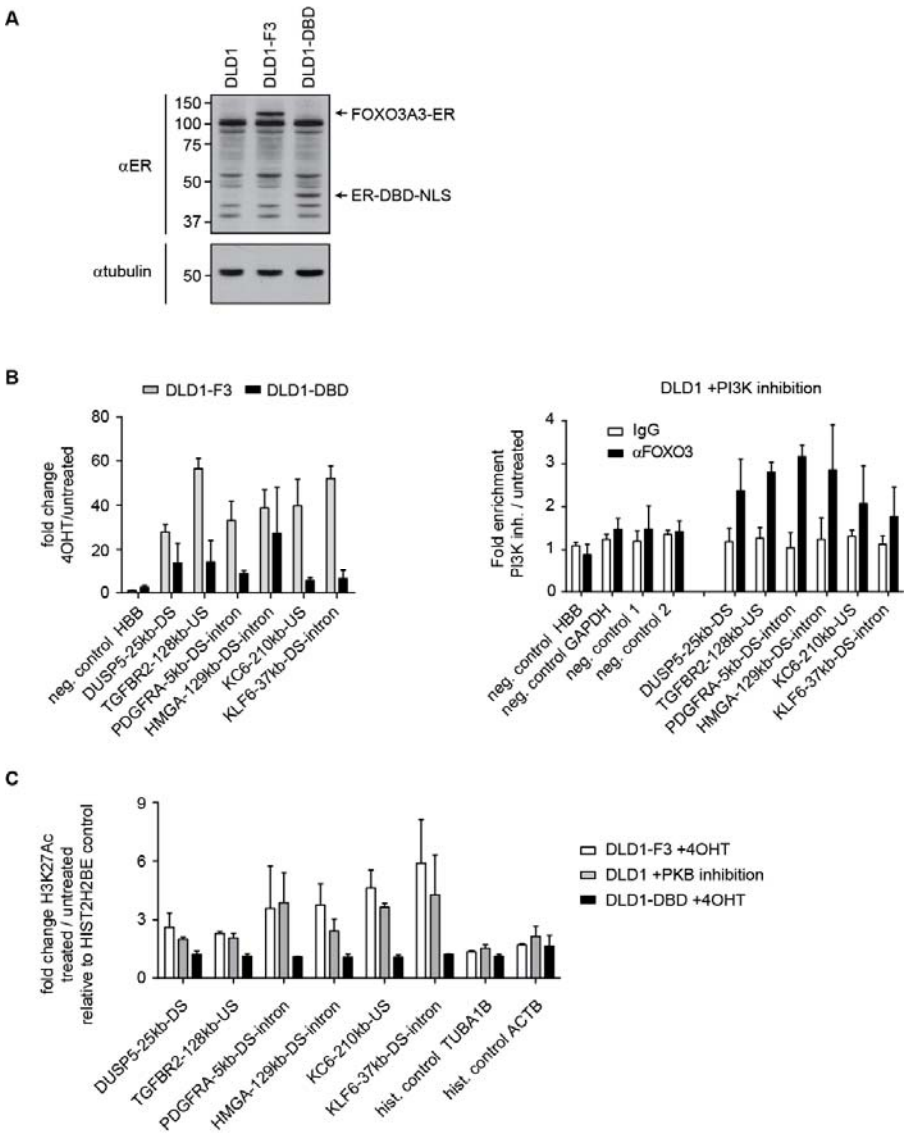

Analysis of binding and effects of ER-DBD fusion protein in DLD1-DBD cells and endogenous FOXO3 activation by PI3K/PKB inhibition. (**A**) Expression levels of full length FOXO3A3 and DBD fusion proteins in DLD1-F3 and DLD1-DBD cells. (**B**) Binding of ER-DBD and endogenous FOXO3 to six regions identified to bind FOXO3A3-ER. Left: ChIP with αER on DLD1-F3 and DLD1-DBD cells before and after 2h treatment with 4OHT. Enrichment was determined by qPCR and fold change relative to untreated is shown (two biological replicates, mean and SEM). Right: ChIP with αFOXO3 on DLD1 cells before and after 1h treatment with PI3K inhibitor. Fold enrichment treated / untreated is shown (three biological replicates, mean and SEM). (**C**) ChIP with αH3K27Ac in DLD1-F3 and DLD1-DBD cells in 16h presence or absence of 4OHT and DLD1 cells with or without PKB inhibition. Enrichment was determined by qPCR for the same six regions and three control regions within the transcribed regions of housekeeping genes TUBA1B and ACTB and histone gene (HIST2H2BE). Values were normalized to HIST2H2BE and fold change relative to untreated is shown (two [DLD1-DBD] or three [DLD1-F3 and DLD1 + PKB inh.] biological replicates, mean and SEM).

Supplementary Figure 8:

A

	DLD1-F3 +4OHT αER	DLD1 PKB inh. αFOXO3	DLD1-DBD +4OHT αER	
DLD1-F3 +4OHT, αER	9152	336	562	n=9932
DLD1 +PKB inh., αFOXO3	319	454	275	n=935
DLD1-DBD +4OHT, αER	539	279	2238	n=2941

B

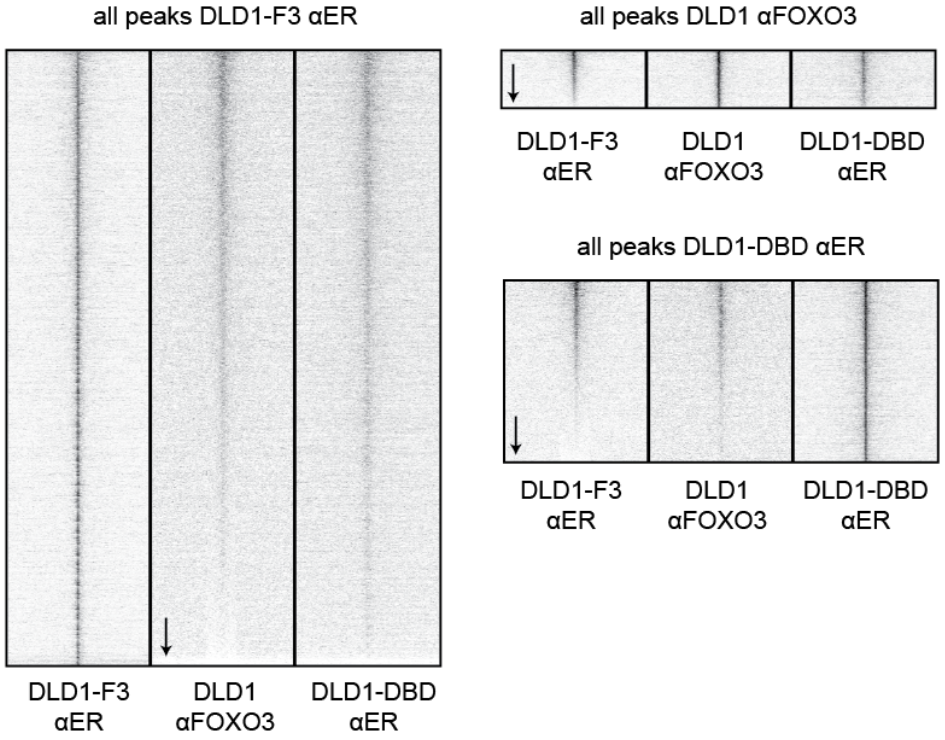

Overlap in ChIP-seq profiles generated from ChIPs with aER in DLD1-F3 and DLD1-DBD cells treated by 4OHT and for endogenous FOXO3 with aFOXO3 in DLD1 cells treated with PKB inhibition. (**A**) Borders of identified peaks were increased to a minimum of 1kb in size surrounding the peak centre and overlap was determined with all three profiles as viewpoint. Table shows overlapping numbers of peaks with grey boxes containing numbers of unique peaks. (**B**) Heat maps of ChIP signal in aER in DLD1-F3 and DLD1-DBD or aFOXO3 in DLD1 cells. Three heat maps show all peaks identified in DLD1-F3, DLD1 and DLD1-DBD respectively and 8 kb regions surrounding these peaks in the other samples. Heat maps are sorted by descending signal in the row indicated by an arrow. Maximum colour intensity corresponds to the 0.98th percentile of the read density distribution.

Supplementary Figure 9:

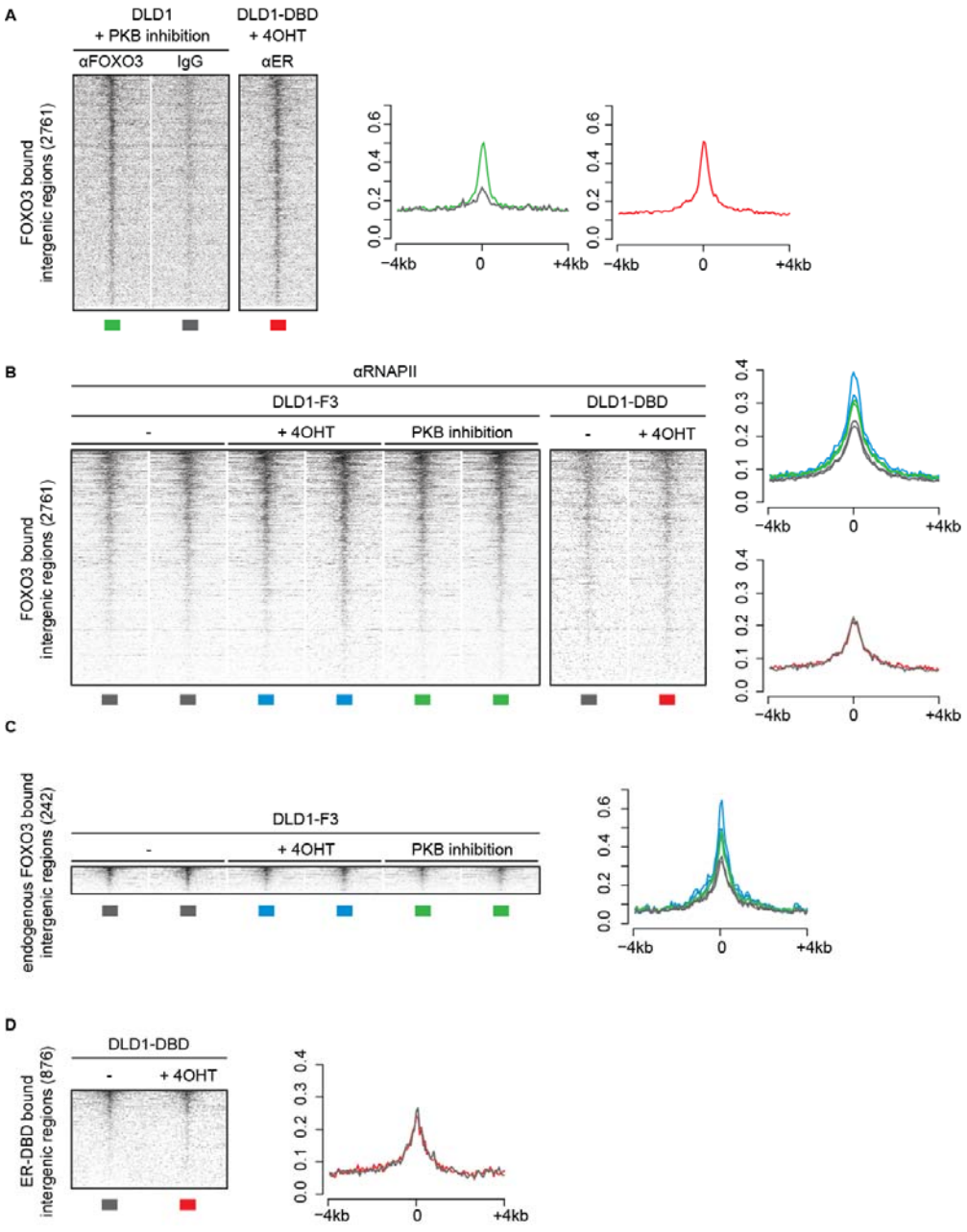

RNAPII occupancy profiles at intergenic FOXO3 bound regions by PKB inhibition and 4OHT treatment in DLD1-DBD cells. (**A**) Heat maps of endogenous FOXO3 occupancy upon PKB inhibition and occupancy of ER-DBD fusion upon 4OHT treatment at all previously identified intergenic FOXO3 bound regions. Each row represents an 8kb region surrounding a FOXO3 peak centre. Graphs represent average signal in the same 8kb regions, colours are below heat maps. (**B-D**) Heat maps of RNAPII occupancy at all FOXO3A3-ER (**B**), endogenous FOXO3 (**C**) and ER-DBD (**D**) intergenic bound regions in indicated samples. Duplicate experiments are shown separately. Graphs represent average RNAPII signal of the same 8kb regions. Signal intensities are normalized for sequencing depth. Maximum colour intensity corresponds to the 0.98th percentile of the normalized read density distribution.

Supplementary Figure 10:

A

	# genes
all genes in analysis	7693
RNAPII >0.5 fold up, 4&24h 4OHT	156
RNAPII >0.5 fold down, 4&24h 4OHT	27
micro-array, up	457
micro-array, down up	627
RNAPII >0.5 fold up, 4h 4OHT	208
RNAPII >0.5 fold down, 4h 4OHT	246
RNAPII >0.5 fold up, 4h PKB inh.	238
RNAPII >0.5 fold down, 4h PKB inh.	178

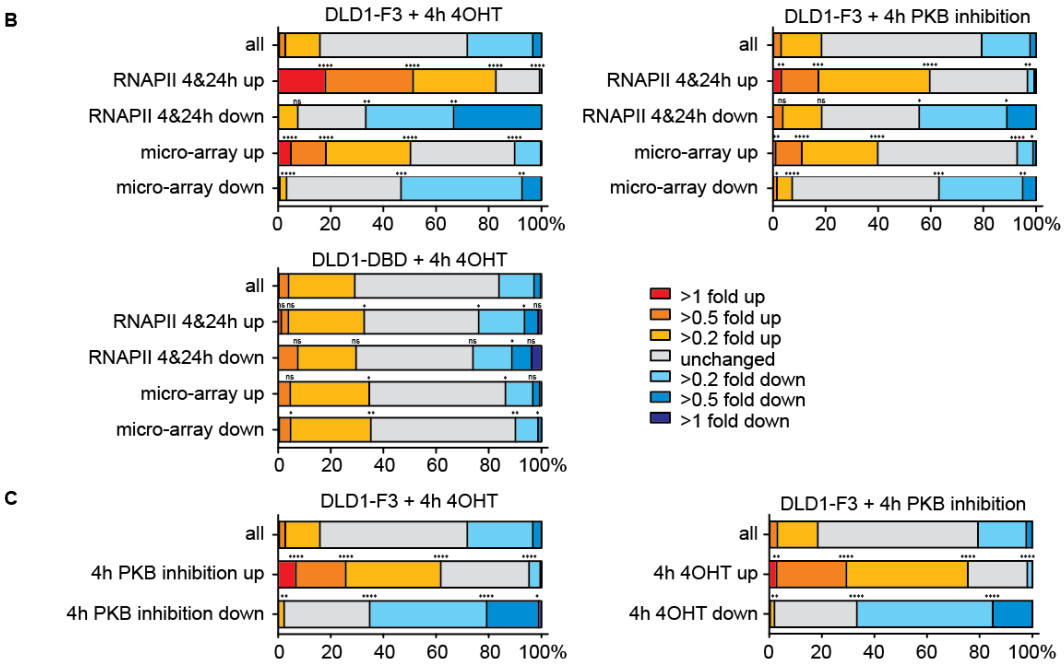

Genome wide induced changes in RNAPII occupancy in replicate experiments. (**A**) Total number of genes included in analysis of overlap. Total number of genes in analysis includes all genes with detectable RNAPII occupancy (>-1.5 NRPKM) in all experiments and excludes genes changed >0.2 fold in DLD1 by 4OHT treatment. Number of genes changed >0.5 (log2) fold by 4h and 24h 4OHT in RNAPII occupancy or >1.3 (linear) fold changed in mRNA levels by treatment in DLD1-F3 cells (as shown in Figure 1, numbers can be smaller since genes below the expression threshold in replicate experiments were excluded from analysis). Average RNAPII occupancy was determined for replicate experiments and numbers of genes changed >0.5 fold upon 4OHT treatment or PKB inhibition. (**B**) Overlap of changes in RNAPII occupancy in replicate experiments with previously identified list of changed genes. Hypergeometric test for overlap subset in changed genes relative to all genes in analysis (ns=p>0.05, * = p<0.05, ** = p<5•10-5, *** = p<5•10-10, **** = p<5•10-15). Status of genes in DLD1-F3 cells with 4h 4OHT treatment, with 4h PKB inhibition and DLD1-DBD cells with 4h 4OHT treatment, all relative to untreated, is shown. Generally, previously identified upregulated genes are also upregulated by 4OHT and PKB inhibition, and vice versa for downregulated genes. Changes in DLD1-DBD cells do not show any similarity with gene status by 4OHT treatment in DLD1-F3 cells. (**C**) Overlap of changes in RNAPII occupancy in replicate experiments with 4OHT treatment or PKB inhibition. Hypergeometric test for overlap subset in changed genes relative to all genes in analysis (ns=p>0.05, * = p<0.05, ** = p<5•10-5, *** = p<5•10-10, **** = p<5•10-15).

Supplementary Figure 11:

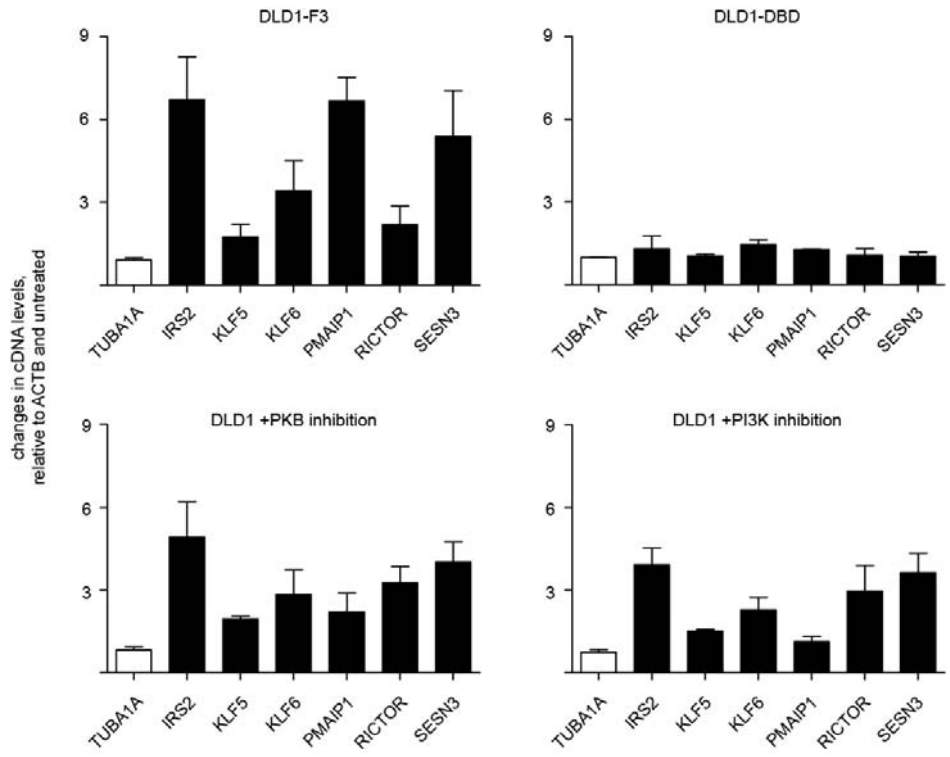

The effects of treatment on target gene expression in DLD1-F3 (with 4OHT), DLD1-DBD (with 4OHT) and DLD1 cells (with PI3K and PKB inhibition). Cells were treated for 8 hours and RNA was purified, followed by cDNA synthesis and qPCR analysis for expression of 6 target genes and 2 controls (TUBA1A and ACTB). Levels were normalized to ACTB and fold change treated over untreated is shown (three biological replicates, mean and SEM).

Supplementary Figure 12:

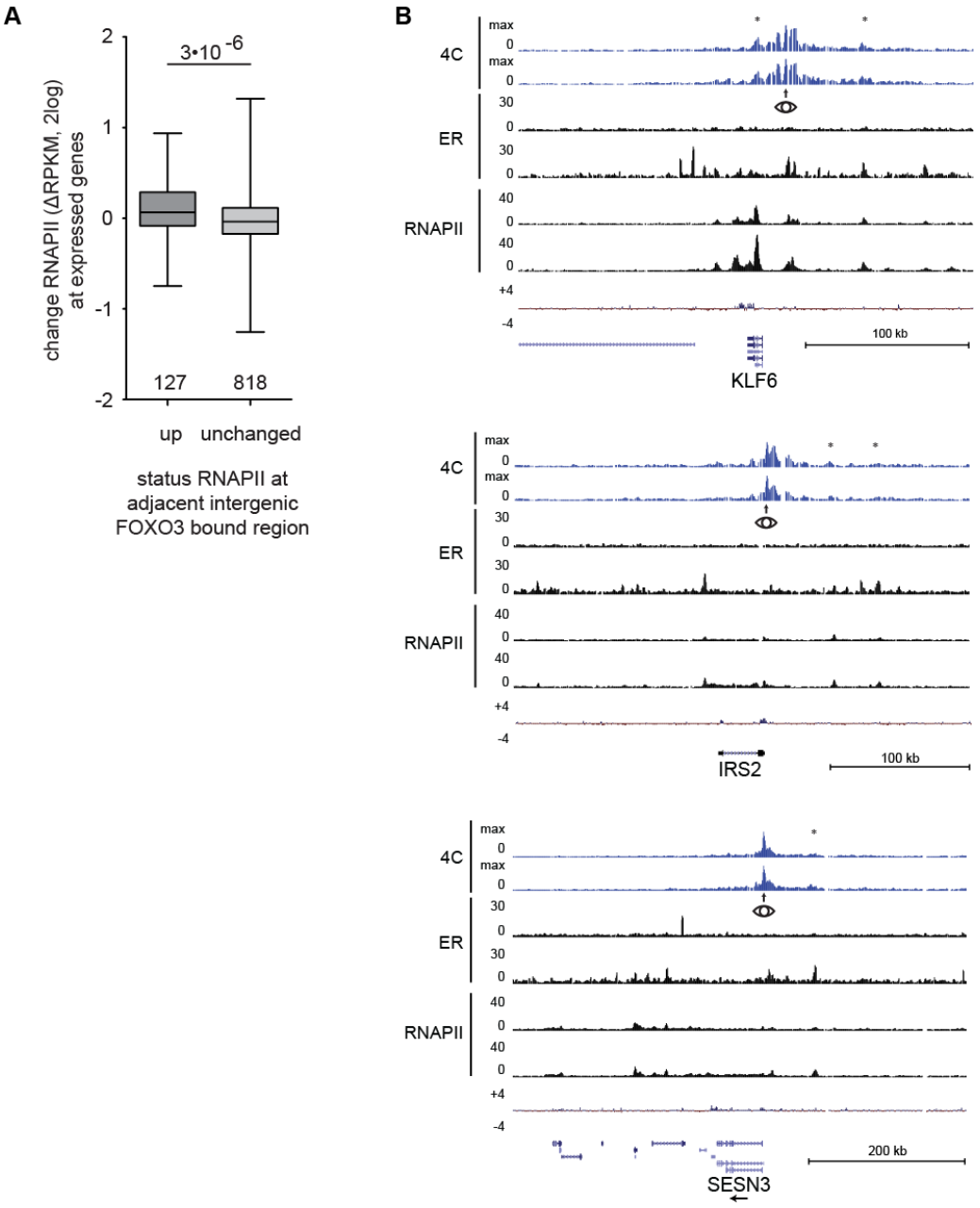

Communication between distal intergenic RNAPII and FOXO3 bound regions and adjacent target genes. (**A**) Status of RNAPII signal at intergenic FOXO3 bound regions in predictive for RNAPII occupancy change of the closest gene. RNAPII signal change was determined for all peaks within 5-100 kb to the TSS of all expressed genes. >0.6 fold induction is cut-off for up regulated RNAPII signal, as determined in Supplementary Figure 6. Fold changes in RNAPII occupancy (DLD1-F3 cells, 4h vs untreated) for genes with unchanged adjacent peak and upregulated adjacent peak are shown (category number indicated, p-value from Mann-Whitney-Wilcoxon test). (**B**) 4C results from regions surrounding KLF6, IRS2 and SESN3, with viewpoints (eye) 20kb upstream for KLF6 and near the TSS for IRS2 and SENS3. Stars indicate the increased 4C signal indicative of looping to the viewpoint.

Supplementary Figure 13:

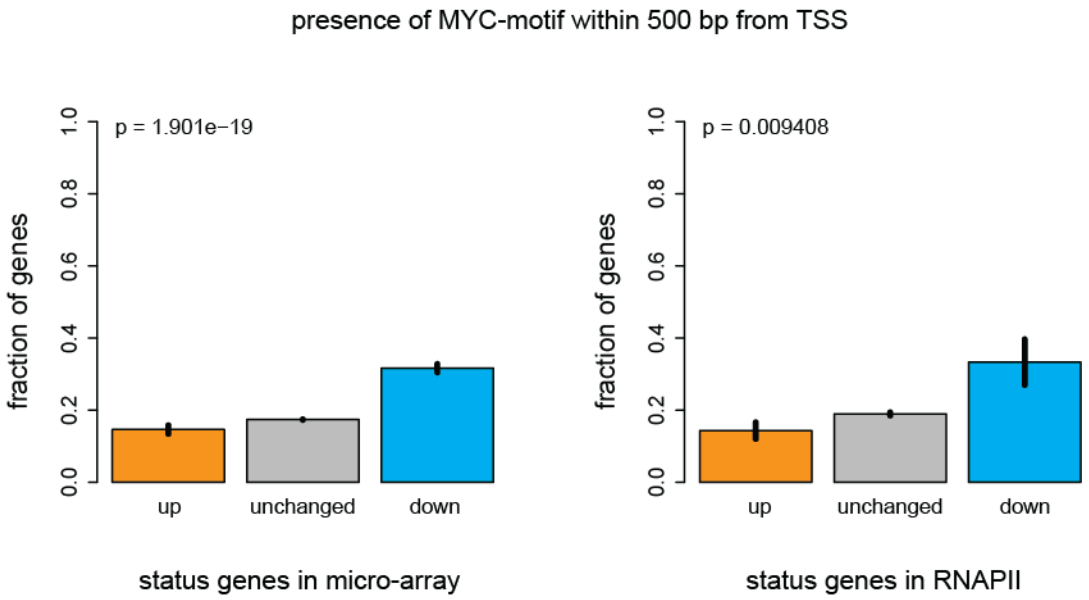

The MYC-DNA binding element is overrepresented in promoters (500bp upstream from TSS) of downregulated genes compared with upregulated genes (p-value from chi-square test up- versus downregulated genes). Cut-off for up and downregulation as determined previously (>1.3 fold [linear] change in micro-array analysis and >0.5 fold [2log] change in RNAPII occupancy).

Supplementary Table Legends

Table S1:
FOXO3 induced transcriptional changes. Table includes all genes for which RNAPII occupancy changes upon addition of 4OHT, ΔNRPKM (changes in normalized read counts per transcript per kb of transcript per million sequencing tags) is >0.5 (log2) fold change in DLD1-F3 4h and/or 24h, and <0.2 in DLD1 4h and 24h relative to untreated. A list of genes for which RNAPII changes are confirmed by micro-array analysis (Ferber et al., 2011) and the numbers changed in this study. GO terms enriched in up- or genes downregulated in RNAP II occupancy, confirmed by micro-array analysis. Last tab contains all genes for which RNAPII occupancy changes upon addition of 4OHT and/or PKB inhibition in replicate experiments (0.5 and 0.2 fold cut-off). Genes with <-1.5 NRPKM in both experiments and >0.2 fold change in DLD1 4h or 24h time points relative to untreated for the first experiment were also excluded from this analysis.

Table S2:
List of FOXO3A3-ER, endogenous FOXO3 and ER-DBD bound regions, including chromosome, start and end, and peak ID.

Table S3:
Sequences of all primers used for ChIP-qPCR, 4C, cloning of luciferase-reporters and qPCR on cDNA.